region is needed. On the other hand, it has been shown in Refs. 6, 11, and, in particular Ref. 12, that if heat conduction is not drastically reduced M_0 (taken at $E_0 \simeq 0$) is supersonic. We conclude, therefore, that for steplike solutions strong reduction of heat conduction is needed.

The importance of radiation-pressure profile modifications lies in the fact that light absorption will be modified. Furthermore, it appears as evident that the thresholds for instabilities, calculated in a WKB-like manner (see, for example, Rosenbluth[13]) for inhomogeneous plasmas, cannot be expected to be correct. As a matter of fact, none of the many instabilities predicted analytically and localized at the critical point has been identified in a convincing manner in a laser plasma experiment. The calculations presented in this paper were performed without absorption. As far as absorption follows Beer's exponential low (e.g., inverse bremsstrahlung), no modifications have been seen because in this case local absorption is very low.

It should be pointed out here that the steplike solution in spherical geometry which is obtained for $M_0 < 1$ has practically the same structure as in the plane case (see Ref. 5) as long as only a narrow region around the critical point is considered. However, no bounded, i.e., physically correct, solution for the electric field is obtained in plane geometry if one starts with $M_0 > 1$, because in this case maintains its initial curvature with growing R, as can be seen from Eqs. (5) and (6′) with $2/R \to 0$. For the formation of the plateau it is essential that (i) M_0 be supersonic and (ii) the flow be divergent.

The authors acknowledge the assistance of Dr. D. Lackner-Russo for her numerical treatment of the equations. They also thank Dr. K. Eidmann and Dr. R. Sigel for discussions of some aspects of the problem treated.

[1]H. Hora, D. Pfirsch, and A. Schlüter, Z. Naturforsch. 22A, 278 (1967).
[2]B. J. Green and P. Mulser, Phys. Lett. 37A, 319 (1971).
[3]D. J. Lindl and P. K. Kaw, Phys. Fluids 14, 371 (1971).
[4]R. E. Kidder, in *Proceedings of Japan-U. S. Seminar on Laser Interaction with Matter*, edited by C. Yamanaka (Tokyo International Book Company, Ltd., Tokyo, 1975), p. 331.
[5]K. Lee, D. W. Forslund, J. M. Kindel, and E. L. Lindmann, Phys. Fluids 20, 51 (1977).
[6]E. Cojocaru and P. Mulser, Plasma Phys. 17, 393 (1975).
[7]P. Mulser and C. van Kessel, Max-Planck-Institut für Plasmaphysik Garching Report No. IPP IV/92, 1976 (unpublished).
[8]J. H. Erkkila, Lawrence Livermore Laboratory Report No. UCRL-51914, 1975 (unpublished).
[9]K. Eidmann, M. H. Key, and R. Sigel, J. Appl. Phys. 47, 2402 (1976).
[10]K. Büchl, K. Eidmann, P. Mulser, H. Salzmann, and R. Sigel, in *Laser Interaction and Related Plasma Phenomena*, edited by H. Schwarz and H. Hara (Plenum, New York, 1972), Vol. 2; J. Shearer, S. W. Mead, J. Petruzzi, F. Rainer, J. E. Swain, and C. E. Violet, Phys. Rev. A 6, 764 (1972); J. F. Kephart, R. P. Godwin, and G. H. McCall, Appl. Phys. Lett. 25, 108 (1974).
[11]J. L. Bobin, Phys. Fluids 14, 2341 (1971).
[12]S. J. Gitomer, R. L. Morse, and B. S. Newberger, Phys. Fluids 20, 234 (1977).
[13]M. N. Rosenbluth, Phys. Rev. Lett. 29, 565 (1972).

Interfacial Surface Energy between the Superfluid Phases of He^3

D. D. Osheroff and M. C. Cross
Bell Laboratories, Murray Hill, New Jersey 07974
(Received 24 January 1977)

We report the first measurements of σ_{AB}, the surface energy associated with the interface between the A and B phases of superfluid ^{3}He as they coexist at T_{AB}. At melting pressure we find $\sigma_{AB} = 6 \times 10^{-6}$ erg cm^{-2} in no magnetic field ($T_{AB}/T_C = 0.79$) rising to $\sigma_{AB} = 1.6 \times 10^{-5}$ erg cm^{-2} in a magnetic field of 4 kOe ($T_{AB}/T_C = 0.5$). Theoretical calculations that we present give an estimate about 50% larger.

At low temperatures liquid He^3 forms two very different superfluid phases.[1-3] In magnetic fields the A phase is always stable near T_c, but below a transition temperature T_{AB} depending both upon field and density, the B phase becomes the stable phase. The phase transition at T_{AB} is first order, and normally is observed to supercool and/or superheat. As a result, experimen-

talists have been able to study both phases over a rather broad temperature interval without changing a single parameter of the system under study. Comparing the properties of the two phases, we can then learn a great deal about them which we could not have learned from either phase alone.

The hysteresis of the A to B phase transition, and in fact the nucleation of the B phase in general, is strongly dependent upon the characteristics of the interface between coexisting regions of He^3-A and He^3-B. This interface is an intrinsic property of bulk liquid He^3, and depends in no way upon the interaction of quasiparticles with surfaces. We report here the first measurements of σ_{AB}, the surface energy associated with this interface, and present theoretical calculations of σ_{AB} which agree reasonably well with the experimental results.

We use an experimental configuration suggested by Leggett[4] to measure σ_{AB} which is analogous to the classical techniques used to measure more conventional surface tensions. Consider a sample of liquid He^3 divided into two separate regions by a thin membrane containing a number of holes of radius r_0. We arrange to have one region filled with He^3-A, and the other filled with He^3-B, with the entire sample at T_{AB}. As we cool the sample, the A-B interfaces at the holes bow toward the A-phase region. The radius of curvature of the interface, r, is related to the difference in free energy of the two phases: $\Delta F_{AB} = 2\sigma_{AB}/r$, where ΔF_{AB} equals $|F_A - F_B|$, the difference in the free energies of the two phases, zero at T_{AB}. Once $r = r_0$, the interfaces will pop through the grid. By knowing ΔF_{AB} when the interfaces pop, we obtain σ_{AB}, since then

$$\Delta F_{AB} = 2\sigma_{AB}/r_0. \tag{1}$$

To determine ΔF_{AB}, note that in a magnetic field, H_0, the free energy of each phase is lowered by $\frac{1}{2}\chi_i H_0^2$, where χ is the magnetic susceptibility of the phase in question. T_{AB} is shifted by the field to a new value, $T_{AB}(H_0)$, where again $\Delta F_{AB}\{T_{AB}(H_0)\}_{H=H_0} = 0$. Since the field has altered ΔF_{AB} (at constant temperature) by $\frac{1}{2}(\chi_A - \chi_B)H_0^2$, we know that in zero field

$$\Delta F_{AB}\{T_{AB}(H_0)\}_{H=0} = \tfrac{1}{2}(\chi_A - \chi_B)H_0^2. \tag{2}$$

From Eq. (2) we can determine ΔF_{AB} at all fields and temperatures, provided we know T_{AB} as a function of $\vec{H}_0$, and $\chi_A - \chi_B$ as a function of temperature.

In our experiment, we use the He^3 melting pressure as a thermometer.[5] By expanding Eq. (2) about T_{AB} and through a change of variables we obtain

$$\Delta F_{AB} = \tfrac{1}{2}(\chi_A - \chi_B)\Delta P(dP_{AB}/dH_0^2)^{-1}. \tag{3}$$

Here P_{AB} is the melting pressure at T_{AB}, and ΔP is the melting pressure interval from P_{AB}, where the interface first reached the grid, to the pressure at which the interface popped through the grid.

To measure σ_{AB}, we have divided the nuclear magnetic resonance (NMR) tail piece of a compressional cooling device into two separate regions by placing a grid containing about 1500 nearly identical holes across the bore of the tail piece in the center of the NMR region. Two separate experiments were performed, one using a 12-μm-thick copper grid containing (41± 3)-μm-diam holes, and the other a 12-μm-thick Mylar grid containing (91± 3)-μm-diam holes. The epoxy tail pieces were mounted with their symmetry axes in the vertical direction, and each had an open cylindrical bore 6 mm in diameter. By using such a large number of holes we were able to reduce the thermal gradients associated with the grid, and could insure that not all the holes were in some way obstructed by solid He^3.

Heaters above and below the NMR region were used to control the distribution of solid He^3 during the experiments. We could prevent solid from forming within the NMR region, or cause solid to form at approximately 1-mm intervals throughout the NMR region by appropriate heating and cooling techniques. Since the temperature of the solid-liquid He^3 interfaces is fixed by the melting pressure, our ability to control the solid distribution allowed us to control the static temperature distribution throughout the cell very precisely. Because of the hydrostatic pressure head of the liquid He^3, the nearly uniform solid distribution enforced a thermal gradient of 3.4 μK/cm in the vertical direction, with the top being warmer than the bottom.

Continuous-wave transverse NMR was used to study the distribution of He^3-A and He^3-B within the NMR region by using the large frequency shift of the A-phase absorption signal to differentiate it from other contributions. A gradient in the static field could be placed along $\vec{H}_0$ (vertically) to provide spatial resolution of the absorption signal. This last technique was useful in understanding the motion of the A-B interface upon warming and cooling.

To measure Δp accurately, the cell was slowly warmed toward T_{AB} until the A-B interface was seen to drop into the NMR region. (Because the $B \rightarrow A$ transition does not superheat at melting pressure, A phase would always nucleate in the upper portion of the cell first.) Then the A-phase absorption signal averaged over the entire region was recorded as a function of melting pressure while the temperature was raised at a rate of 1 to 3 μK/min. Once the A-B interface dropped below the NMR region, the sample was cooled back before the B-phase region had been destroyed entirely. Finally the average signal was recorded again while cooling.

Typical signals recorded in the manner described above are shown in the inset to Fig. 1. Upon warming (lower curve), the A-B interface dropped down into the NMR region at C, reached the grid at D, passed through the grid at E, and dropped below the NMR region at F. The interval over which the interface remained on the grid, $D-E$, varied from about 1 to 2 μK for both grids in a nonsystematic manner. The temperature interval corresponding to $C-F$ was generally about equal to the temperature difference from the top to the bottom of the NMR region. We therefore conclude that the ΔP corresponding to $D-E$ is not associated with σ_{AB} but results from the small disturbance in the thermal gradient caused by the presence of the grid. The ease with which the interface appeared to pass through the grid indicates how easily the A phase can be nucleated from the B phase upon warming.[6]

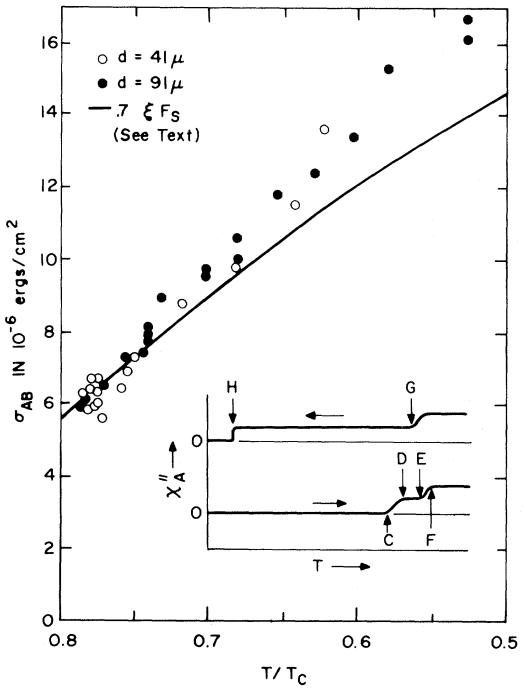

FIG. 1. The interfacial surface energy between He^3-A and He^3-B at melting pressure. The solid line is for comparison with theory which predicts $\sigma_{AB} \approx 1.1 \xi F_s$. The inset shows typical data from which σ_{Ab} is determined. The labeled points are explained in the text.

Upon cooling (upper trace in the inset to the figure) the A-B interface is seen to rise up to the grid at G, and finally pop through the grid at H. The temperature interval corresponding to $G-H$ was typically 8 μK for the 91-μm grid, and 18 μK for the 41-μm grid. To compensate for thermal lag in the motion of the interface, P_{AB} was defined as $\frac{1}{4}(D+E)+\frac{1}{2}G$. The pressure interval in Eq. (3) is then $\Delta P = H - \frac{1}{4}(D+E) - \frac{1}{2}G$. The point H reproduced itself during a single run to better than $\pm$ 100 nK, but because of the thermal lag in the motion of the interface, ΔP typically fluctuated by $\pm$ 4% for a given value of T_{AB}.

Data of the sort described above were obtained in a series of magnetic fields corresponding to values of T_{AB}/T_c from 0.78 to 0.50. Over this interval, values of ΔP decreased by about 25% as the temperature T_{AB} was lowered. Surface energies were calculated from (1) and (3) using the dynamical values of χ_B/χ_N measured by Corruccini and Osheroff[7] assuming the normal-state susceptibility to be[2] $\chi_N = 1.12 \times 10^{-7}$. Values of σ_{AB} determined from the data are shown in the figure as a function of T/T_c, and the reader is reminded that H_0 is an implicit variable as well. We observe no systematic variation between the 41-μm data and the 91-μm data. Furthermore, we saw no systematic dependence of the results upon the distribution of solid He^3 within the cell. For these reasons we believe estimates of σ_{AB} based on averages of the values shown in the figure should be accurate to better than 5%.

We have calculated σ_{AB} as the additional free energy due to the requirement that the gap matrix, $\vec{\vec{d}}$, changes continuously across the interface. This energy is the sum of the bending energy (the energy resulting from gradients in $\vec{\vec{d}}$) and the extra free energy of the nonequilibrium states passed through.

To determine the path in the multidimensional space of the components of $\vec{\vec{d}}$ which minimizes σ_{AB} is exceedingly difficult. Instead, we use physical arguments to determine a suitable path. We know that $\sigma_{AB} \sim (F_s f)^{1/2} \xi$, where F_s is the difference between the normal phase and superfluid free energies at T_{AB}, f is the maximum addition-

al free energy along the path, and ξ is the temperature-dependent coherence length [we choose the normalization $\xi^2 = 7\zeta(3)\hbar^2 v_F^2/48\pi^2 k_B^2 T_c^2(1-T/T_c)$]. We take the path to be A-P-B, where A is the Anderson-Brinkman-Morel state, B is the Balian-Werthamer state, and P is the planar, or two-dimensional, state (for a description of these states see Ref. 1). The peak height f is then the P-A free energy difference. This difference is zero in the weak-coupling limit, and small if the strong-coupling corrections are not too large. Thus we take

$$\vec{d} = \frac{\Delta}{\sqrt{2}} \begin{pmatrix} \cos\chi & 0 & 0 \\ 0 & \cos\theta\cos\chi & 0 \\ -i\sin\theta\cos\chi & 0 & \sqrt{2}\sin\chi \end{pmatrix}.$$

Here $\chi = 0$, $\pi/2 \geq \theta \geq 0$ defines states from A to P; $\theta = 0$, $0 \leq \chi \leq \sin^{-1}(1/\sqrt{3})$ defines states from P to B; Δ is the energy gap, taken to be constant; and the $\hat{x}$ direction in orbit space is normal to the interface. This orientation minimizes at each point the bending-energy terms with respect to rotations of $\vec{d}$ in spin and orbit space.[8]

Expressions for free energies at arbitrary temperatures including strong-coupling corrections are not known. However, weak-coupling free-energy differences between phases, when expressed as a fraction of F_s, are pressure independent at constant T/T_c and also nearly temperature independent. Therefore along the T_{AB} line, where strong-coupling corrections just cancel the weak-coupling free-energy difference between the A and B phases, the strong-coupling contributions must also be roughly constant when expressed in the same manner. We therefore calculate σ_{AB} by determining the ratio $\sigma_{AB}/F_s\xi$ at the polycritical point, and use this ratio as a guide to the corresponding ratio at melting pressure.

At the polycritical point, we use a fourth-order Ginzburg-Landau expansion for the free energies,[9,10] and determine the five fourth-order free-energy invariants in superfluid He^3 from spin fluctuation theory.[11] This theory is quite successful in describing the ratios of the free energies of the various phases.[3] Bending-energy expressions in the Ginzburg-Landau region are well known.[1,3] Finally, the sum of the bulk and bending energies integrated over the path is minimized. In this manner we find $\sigma_{AB} = 1.1\xi F_s$.

To compare the experimental results with the theory, we determine F_s by integrating the specific heats of the superfluid and normal phases twice from T_c downward using the polynomial expressions with which Halperin fitted his data.[5,12]

In the figure we show as a solid line $0.7\xi F_s$, obtained from the integrated specific heats described above. By comparing this line with the experimental results, we see that the theoretical prediction that $\sigma_{AB} \simeq 1.1\xi F_s$ is reasonably accurate, particularly considering the uncertainties which exist in determining the strong-coupling effects and the extrapolations which we have made in both temperature and pressure to make the comparison.

Our results do not resolve the B-phase nucleation problem. Based on our measurements, we estimate the energy necessary to create a sufficient bubble of He^3-B in bulk He^3-A to cause nucleation is typically several million times $k_B T$. Yet, since T_{AB} is depressed by the presence of surfaces, it seems unlikely that surfaces could promote B-phase nucleation. It has recently been suggested[13] that B phase could perhaps nucleate from extended signularities in bulk A phase. With our results, calculations may now test this hypothesis.

We wish to acknowledge contributions to the theoretical work presented here by W. F. Brinkman and useful and stimulating conversations regarding the experiment with A. J. Leggett and N. D. Mermin. We also wish to thank W. O. Sprenger for his technical support.

[1]A. J. Leggett, Rev. Mod. Phys. 47, 131 (1975).

[2]J. C. Wheatley, Rev. Mod. Phys. 47, 415 (1975).

[3]P. W. Anderson and W. F. Brinkman, in *The Helium Liquids*, edited by J. G. M. Armitage and I. E. Farquhar (Academic, London, 1975).

[4]A. J. Leggett, private communication.

[5]W. P. Halperin, C. N. Archie, F. B. Rasmussen, T. A. Alvesalo, and R. C. Richardson, Phys. Rev. B 13, 2124 (1976).

[6]Calculations show this nucleation may result from surface irregularities of magnetic impurities in the chamber walls which stabilize the A phase at low temperatures.

[7]L. R. Corruccini and D. D. Osheroff, Phys. Rev. Lett. 34, 695 (1975). Thermodynamical measurements (Ref. 5) support our use of the NMR measurements of χ_B/χ_N rather than an extrapolation to melting pressure of the larger static susceptibility differences (see for instance Ref. 2).

[8]A complete description of the theoretical calculation including consequent boundary conditions on $\hat{n}$, $\vec{d}$, and $\hat{l}$ will be reported by M. C. Cross (to be published).

[9]W. F. Brinkman and P. W. Anderson, Phys. Rev. A

8, 2732 (1973).
[10]N. D. Mermin and G. Stare, Phys. Rev. Lett. 30, 1135 (1973).
[11]W. F. Brinkman, J. Serene, and P. W. Anderson, Phys. Rev. A 10, 2386 (1974).
[12]W. F. Halperin, Ph.D. thesis, Cornell University, 1974 (unpublished).
[13]N. D. Mermin, to be published.

Bicritical and Tetracritical Behavior of $GdAlO_3$

H. Rohrer and Ch. Gerber
IBM Zurich Research Laboratory, 8803 Rüschlikon, Switzerland
(Received 4 February 1977)

We have experimentally investigated the phase diagram of antiferromagnetic $GdAlO_3$ near its spin-flop multicritical point (T_M, H_M) in the three-dimensional space spanned by the uniform fields $H_\parallel$ and $H_\perp$ and the temperature T. In the $H_\parallel$-T plane, (T_M, H_M) appears as a bicritical point, but as a tetracritical point in the $H_\perp$-T plane. The approach of all six boundaries to (T_M, H_M) is described by a single exponent $\psi = 1.17 \pm 0.02$. This implies crossover exponents $\varphi = 1.17 \pm 0.02$ and $\varphi_v = \pm 0.03$ in excellent agreement with renormalization group theory.

The work on bicritical and tetracritical points by Fisher and Nelson[1] and Aharony and Bruce[2] has opened an area of intensive theoretical investigations of such points.[3] Experimental studies have, however, been confined to bicritical points.[4,5] The reason is that systems with the appropriate quadratic[6] or quartic[2,3] anisotropies required to yield a tetracritical point with three ordered phases of different symmetry are not very abundant. Recently, Mukamel[7] has proposed some planar antiferromagnets with possible tetracritical points at zero field. In some of these systems, a tetracritical behavior is expected only for distinct field directions, whereas for all other directions, it appears as a bicritical point. Thus, the type of critical behavior depends on the direction of the applied field.

The situation is similar in antiferromagnets with a spin-flop multicritical point at finite fields.[3] The present work verifies such tetracritical behavior and is the first experimental observation bearing on φ_v, the crossover exponent associated with cubic anisotropy. In addition, the bicritical lines have been obtained for considerably improved alignment.[4] Figure 1 shows the phase diagram of a uniaxial antiferromagnet in the space of uniform fields $H_\parallel$ and $H_\perp$ and the temperature T.[3,4] $H_\parallel$ is applied along the easy axis of magnetization, $H_\perp$ perpendicular to it. The shelf of first-order spin-flop (SF) transitions touches the surface of second-order transitions to the paramagnetic (PM) state in a multicritical point (T_M, H_m). In the $H_\parallel$-T plane, we find the well-known bicritical behavior,[1,2] where the first-order SF transition line meets the antiferromagnetic (AF)-PM and flop (FL)-PM λ lines. In the $H_\perp$-T plane [or, more precisely, in the plane tangent to the SF transition shelf at (T_M, H_M)], this point is tetracritical and the four critical lines meet tangentially: the two spin-flop critical lines T_c^{SF} bounding the SF transition shelf and the two PM transition lines T_c^{PM}. It should be noted that this is a special type of tetracritical point with four Ising-like critical lines. For other tetracritical points, the SF transition shelf of Fig. 1 can be parallel to $H_\parallel$. Bicritical behavior is then found in the $H_\perp$-T plane.

For $GdA10_3$ with orthorhombic anisotropy,[8] Fig. 1 only applies if $H_\perp$ is applied along the axis of

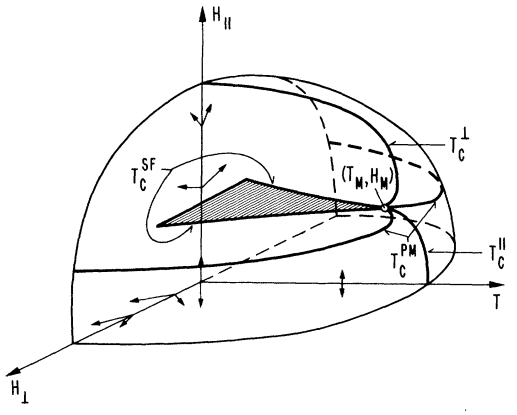

FIG. 1. Phase diagram of a uniaxial antiferromagnet in the space of uniform fields $H_\parallel$ and $H_\perp$ and temperature T. The bicritical lines $T_c^\perp$ and $T_c^\parallel$ and the tetracritical lines T_c^{SF} and T_c^{PM} meet tangentially at the multicritical point (T_M, H_M) (open circle). The shaded area is the shelf of first-order spin-flop transitions.